Research Square

Preprints are preliminary reports that have not undergone peer review.
They should not be considered conclusive, used to inform clinical practice,
or referenced by the media as validated information.

Interactive effects of CO2 concentration and temperature on photosynthesis and growth of cultivated Ulva prolifera germling clusters

Kaho Yamaha
Nagasaki University
Gregory N. Nishihara
greg@nagasaki-u.ac.jp

Nagasaki University
Yoichi Sato
Algal Research Innovation Centre (ARIC), Riken Food Co. Ltd
Eri Inomata
Algal Research Innovation Centre (ARIC), Riken Food Co. Ltd

Research Article

Keywords: CO2 enrichment, Temperature, Terrestrial aquaculture, Relative growth rate, Photosynthesis, Carbon concentrating mechanism

Posted Date: September 23rd, 2025

DOI: https://doi.org/10.21203/rs.3.rs-6725046/v2

License: This work is licensed under a Creative Commons Attribution 4.0 International License.
Read Full License

Additional Declarations: No competing interests reported.

Title: Interactive effects of CO_2 concentration and temperature on photosynthesis and growth of cultivated *Ulva prolifera* germling clusters

Author: Kaho Yamaha[1], Gregory N. Nishihara[2,3], Yoichi Sato[4,5], Eri Inomata[4]

Affiliation:

1 Graduate School of Fisheries and Environmental Sciences, Nagasaki University, Nagasaki, Japan, 852-8521

2 Organization for Marine Science and Technology, Nagasaki University, Nagasaki, Japan, 852-8521

3 Institute for East China Sea Research, Nagasaki University, Nagasaki, Japan, 951-2213

4 Algal Research Innovation Centre (ARIC), Riken Food Co. Ltd., Miyagi, Japan 981-1204

5 Nishina Center for Accelerator-Based Science, RIKEN, Saitama, Japan, 351-0198

*Corresponding author: Gregory N. Nishihara (greg@nagasaki-u.ac.jp)

Abstract

Terrestrial aquaculture of the economically important green seaweed *Ulva prolifera* offers potential for stable production but requires optimization due to high operational costs. While CO_2 enrichment can enhance growth, its interaction with temperature is not fully quantified for the germling cluster cultivation method. The interactive effects of dissolved CO_2 concentration (0.07 to 12 µatm) and temperature (10, 20, and 30 °C) on the net photosynthetic rate (NPR) and relative growth rate (RGR) of cultivated *U. prolifera* germling clusters under controlled laboratory conditions (150 to 200 µmol photons m^{-2} s^{-1}) were investigated. NPR was measured via oxygen evolution in short-term incubations, and RGR was determined from wet weight changes over 6-day batch cultures with daily medium exchange. A generalized additive model was used in the analysis. RGR peaked under different CO_2 concentrations that varied with temperature, reaching a maximum value of 0.40 at 0.40 µatm for the 10 °C treatment, 0.69 at 1.41 µatm for the 20 °C treatment, and 0.67 at 1.77 µatm for the 30 °C treatment. In contrast, NPR showed complex responses, generally reaching a plateau above 5 µatm at 10 °C and 20 °C, but remaining relatively high across all CO_2 levels at 30 °C. The discrepancies observed

regarding the response of photosynthesis and growth to CO_2 concentrations indicates that factors beyond immediate carbon fixation (e.g., the importance of time-scales) influence overall biomass accumulation under varying CO_2 (i.e., pH) conditions.

Keywords: CO_2 enrichment, Temperature, Terrestrial aquaculture, Relative growth rate, Photosynthesis, Carbon concentrating mechanism

Introduction

Species of the genus Ulva are ecologically significant green macroalgae in coastal ecosystems and hold increasing economic importance for food, feed, bioremediation, and potential biofuel applications (Bolton et al. 2016; Bruhn et al. 2011). However, their ability to form large-scale green tides also necessitates research into management and use (Liu et al. 2013; Ye et al. 2011). Among these, *Ulva prolifera* O.F. Müller, a filamentous species typically inhabiting brackish estuaries (Hiraoka & Higa 2016), is traditionally consumed in East Asia and has a history of cultivation [e.g., in Yoshino River estuary, Tokushima, Japan (Watanabe et al. 1999; Shimada 2012).] Nevertheless, the stability of seaweed production globally, including that of *U. prolifera*, is threatened by the impacts of climate change, especially rising water temperatures and changes to the estuarine environment (e.g., Harley et al. 2012; Gao et al. 2015). Climate change related impacts can be expected to lead to declines in production yield (e.g., Hiraoka et al. 1999; Sato et al. 2021).

To ensure stable production amidst environmental variability, terrestrial aquaculture systems offer greater control over cultivation conditions (Mantri et al. 2021; Lawton et al. 2021). A key development for *U. prolifera* is the *germling cluster* method, which utilizes aggregated asexual germlings, thereby circumventing the risk of maturation and reproduction that is often induced by factors like elevated temperature and enabling continuous vegetative cultivation (Hiraoka & Oka 2008; Dan et al. 1998; Sato et al. 2021). Despite these advantages, the significant financial investment required for terrestrial infrastructure and operation makes maximizing biomass yield per unit area a critical factor for economic feasibility (Milledge & Harvey, 2016; Sato 2024). Consequently, identifying and optimizing the environmental parameters that govern growth rates is imperative.

Optimizing production requires understanding the physiological response *Ulva prolifera* to key environmental factors. While adapted to fluctuating estuarine conditions and capable of

surviving temperatures down to 5 °C as well as wide salinity ranges (Xiao et al. 2016), its growth and photosynthetic rates are maximized within narrower windows. Optimal temperatures of *U. prolifera* are often reported around 20 °C for growth and 14 to 27 °C for photosynthesis (Xiao et al. 2016; Cui et al. 2015). Similarly, while tolerant of varying irradiance, light saturation levels differ for growth (> 67 µmol photons m^{-2} s^{-1}; Hiraoka et al. 2020) and photosynthesis (126 to 683 µmol photons m^{-2} s^{-1}; Xiao et al. 2016) and may be reflecting differences in the strains examined, experimental artefacts, and the different time scales involved. Importantly, temperature, high light intensity, and low salinity can induce maturation, which can be undesirable in a production setting (Dan et al. 1998; Jiang et al. 2024; Lin et al. 2011). Hence the difficulty in achieving a stable environment that can prevent maturation in aquaculture systems where temperature and light fluctuate. Therefore, it is desirable to develop methodology for controlled environments or alternative methods to enhance yield.

Carbon dioxide enrichment is one potential strategy to enhance macroalgal productivity, particularly in controlled land-based systems where atmospheric exchange may be limited or where boosting growth beyond ambient CO_2 levels is possible (Gao et al. 1991; Zou 2005; Figueroa et al. 2021). Previous studies have demonstrated that elevated CO_2 can boost physiological performance and growth of *U. prolifera* (Xu & Gao 2012; Sun et al. 2021; Wang et al. 2021); however, given that temperature strongly influences the photosynthetic and growth rates of this species (Xiao et al. 2016), understanding the interactive effects of CO_2 supply and temperature is crucial for developing effective cultivation protocols. The optimal CO_2 concentration for maximizing growth may vary depending on the cultivation temperature, yet this interaction has not been sufficiently quantified for *U. prolifera* germling clusters used in aquaculture. Therefore, we hypothesized that the CO_2 concentration yielding maximum relative growth rate (RGR) for *U. prolifera* germling clusters depends on water temperature. We aimed to determine the interactive effects of dissolved CO_2 concentration (ambient to 12 µatm) and temperature (10, 20, and 30 °C) on the net photosynthetic rate (NPR) and relative growth rate (RGR) of *U. prolifera* germling clusters, to identify optimal conditions for enhancing productivity in terrestrial aquaculture.

Materials and Methods

Ulva prolifera germling cluster production and maintenance

The *U. prolifera* strain used in this study, originally collected from the Takeshima River, Shimanto City, Kochi Prefecture, Japan, is an asexual variant selected for high temperature tolerance suitable for terrestrial aquaculture (Sato et al. 2021). Stock cultures were maintained via successive cultivation at the Yuriage Factory of Riken Food Co., Ltd., Natori city, Miyagi Prefecture, Japan. Germling clusters were produced following Hiraoka and Oka (2008) by aggregating germlings released after asexual reproduction. For experiments conducted at Nagasaki University, we shipped clusters (approximately 1 cm in diameter) in 1 L bottles with sterilized seawater maintained at about 10 °C. Upon arrival, clusters were acclimated and pre-cultured at the Institute for East China Sea Research, Nagasaki University, Nagasaki, Japan (ECSER).

For the NPR experiment we pre-cultured the germling clusters. Germling clusters were transferred to a 34.7 L container with 15 L of sterilized artificial seawater (SF-1, Osaka Yakuken, Osaka, Japan) enriched with 15 mL of nutrient stock (NORISEED-1L, Daiichi, Kumamoto, Japan). Temperature was maintained at 20 °C using a chiller (ZC-200α, ZENSUI, Osaka, Japan) in a water bath. Cultures were incubated for 2 days under a 12h:12h light:dark cycle at 150 µmol photons m^{-2} s^{-1} (LED: L200V2-D-HMW-50K, NICHIDO, Osaka, Japan) with aeration with ambient air, until the germling clusters reached approximately 1 g wet weight (g_{ww}). Cultures were maintained under continuous low light (< 20 µmol photons m^{-2} s^{-1}) overnight before experiments.

For the RGR experiment, the pre-culturing and experiments were conducted at the Yuriage Factory using germling clusters maintained as described above.

CO_2 enriched culture medium preparation

For the NPR and RGR experiments, CO_2 enriched media were prepared shortly before use. Sterilized seawater (artificial seawater for NPR experiments, filtered natural seawater for RGR experiments) was poured into a 500 mL flask and vigorously aerated with pure CO_2 gas (100%) for about 10 seconds using an air tube and air stone. This stock solution was then diluted with non-aerated sterilized seawater to achieve target CO_2 concentrations. Dissolved CO_2

concentration was measured using a portable meter (CGP-31, DKK-TOA, Tokyo, Japan), and pH (NBS scale) was measured using a pH meter (NPR: WQ-320, HORIBA, Kyoto, Japan; RGR: D-52S, HORIBA, Kyoto, Japan) before and after experimental incubations or during daily media changes. Target CO_2 concentration ranges are specified below for each experiment since it was extremely difficult to consistently create exact concentrations of the CO_2 media.

Response of NPR to CO_2 and temperature

NPR was measured using 1 g_{ww} germling clusters that were pre-cultured as described above. Single clusters were secured with a net inside 100 mL BOD bottles filled with prepared medium at one of three target temperatures (10, 20, and 30 °C) and one of eight target CO_2 concentration ranges (Table 1). Five replicate bottles were used per CO_2 level at each temperature. The mean CO_2 concentration measured before and after the incubation was used as the representative value for statistical analysis. The CO_2 concentrations were converted from values provided by the CGP-31 meter to µatm (Table 1) using the x2pCO_2 function of the R package seacarb (Weiss 1974; Dickson et al. 2007; Gattuso et al. 2024).

Bottles were placed in a temperature-controlled glass water bath illuminated from above at 200 µmol photons m^{-2} s^{-1} (LED: L200V2-D-HMW-50K, NICHIDO). Light intensity was measured using a planar quantum sensor (LI-192 connected to LI-1400, LI-COR, Lincoln, NE, USA). Clusters were acclimated in the bottles for 16 minutes. Dissolved oxygen (DO) concentration was measured every 2 minutes after acclimation for 24 minutes using a BOD sensor connected to a meter (ProSolo with 626660 sensor, Xylem, Kanagawa, Japan). Water was continuously stirred using the integrated stirrer of the BOD sensor. The net used to secure the cluster prevented any movement of the cluster and damage that could have occurred due to the impeller of the stirrer.

NPR was calculated from the linear rate of DO increase over the measurement period. The slope (b_1, mg O_2 L^{-1} min^{-1}) was determined by linear regression (Eq. 1).

$$y = b_0 + b_1\tau \quad (1)$$

Where, b_0 is the intercept and τ is time in minutes. NPR was calculated with Eq. 2.

$$NPR = \frac{b_1 V}{W} \quad (2)$$

Where, V is the volume of the BOD bottle and W is the wet-weight of the germling cluster. The units of NPR are in µg O_2 g_{ww}^{-1} min^{-1}.

Response of RGR to CO_2 and temperature

RGR experiments were conducted at the Yuriage Factory using filtered natural seawater (salinity 28 to 34 psu, measured prior to each experiment) enriched with 1/2 strength PES medium. Clusters (initial weight of about 1 g_{ww}) were incubated individually in 1 L flasks containing 1,100 mL of medium with target CO_2 concentrations. Eight target CO_2 concentrations were used for the 10 °C and 30 °C experiments, whereas nine target concentrations were used for the 20 °C experiment (Table 2). The mean CO_2 concentration measured across daily media changes over a 5 to 6 day period was used as the representative value. The CO_2 concentrations were converted from values provided by the CGP-31 meter to µatm using the x2pCO_2 function of the R package seacarb (Weiss 1974; Dickson et al. 2007; Gattuso et al. 2024) and for this experiment assuming a mean salinity of 31 psu and an atmospheric pressure of 101.35 kPa.

Flasks were incubated at 10, 20, or 30 °C inside incubators (CN–40A, MITSUBISHI, Tokyo, Japan) under a 12h:12h light:dark cycle at 150 µmol photons m^{-2} s^{-1} (Light source: 3LH–64, Nippon Medical & Chemical Instruments, Osaka, Japan). Flasks were continuously stirred with magnetic stirrers (BIG Squid White, IKA, Osaka, Japan). The medium was completely replaced daily, at which time CO_2 and pH were measured. Wet weight was measured after blotting dry with a paper towel every other day following Sato et al. (2021).

$$RGR = \frac{\ln W_\tau - \ln (W_0)}{\tau} \quad (1)$$

Where, W_τ is the wet weight in grams after τ = 5 or 6 days and W_0 is the initial wet weight at day 0.

Statistical analysis

All statistical analyses were performed using R version 4.4.2 (R Core Team 2024). The effects of CO_2 concentration and pH on NPR and RGR, nested within temperature treatments, were analyzed using hierarchical generalized additive models (GAMs) following recommendations of

Pedersen et al. (2019). Each model included a global smoother (P-spline) across all temperatures and temperature-specific smoothers (P-spline interacting with temperature factor). Basis functions were chosen based on expected complexity (e.g., 10 basis functions for all smoothers of NPR, 7 basis functions for all smoothers of RGR). A Gamma error distribution with a log-link function was assumed for both NPR and RGR.

Models were fitted using a Bayesian approach via Hamiltonian Markov Chain Monte Carlo (MCMC) with the brms package (Bürkner 2017, 2018). Default weakly informative priors (t-distributions) were used for model coefficients and smoothing parameters. Model comparison between a null model (global smoother only) and the full hierarchical model (global and temperature-specific smoothers) was performed using leave-one-out cross-validation (LOO-CV) via the loo package (Vehtari et al. 2017) to confirm the significance of temperature-specific effects. Posterior distributions were visually inspected for convergence. Model predictions and 95% highest density credible intervals (HDCI) were extracted from the posterior distributions.

Results

Response of NPR to CO_2 concentration and pH fraction

The NPR of *U. prolifera* germling clusters varied depending on both temperature and CO_2 concentration and pH; the model that included temperature specific effects better predicted the observations when compared to a global model averaged over the temperatures (Fig. 1). The difference in the leave-one-out cross validation of the NPR vs. CO_2 analysis was -154 $\pm$ 9.9 (expected value ± 1 standard error) in favor of the more complex model. When the covariate was pH the values was -150.2 ± 10.2 and favored the more complex model. Overall NPR was substantially lower at 10 °C compared to 20 °C and 30 °C, where rates were comparable. The mean and one standard deviation of the NPR averaged over CO_2 concentration at 10 °C was 0.65 ± 0.25 (n = 38), 1.87 ± 0.33 (n = 39) at 20 °C, and 1.94 ± 0.30 (n = 40) at 30 °C. The model expectations exhibited different patterns across temperatures and the variability in NPR increased with increasing NPR. Based on expectations, the predicted NPR was highest at 0.69 µatm with a value of 0.84 (0.77 to 0.90) mg O_2 g_{ww}^{-1} min^{-1} (expected value and the 95% HDCI) in the 10 °C treatment (Fig. 1A). In the 20 °C and 30 °C treatments, the response did not appear curvilinear (Fig. 1B and C) and the highest NPR occurred at the model origin. For the 20 °C treatment the NPR was highest at 0.07 µatm and was 2.10 (1.92 to 2.29) mg O_2 g_{ww}^{-1} min^{-1} (Fig.

198 1B). In the 30 °C treatment, NPR was highest at 0.07 µatm with a value of 1.98 (1.83 to 2.13)
199 mg O_2 g_{ww}^{-1} min^{-1}; however, NPR remained relatively high across the range of CO_2 examined
200 (Fig. 1C).

201 When analyzed against pH, the predicted NPR response generally increased then decreased
202 across a gradient of pH at 10 °C and 20 °C, however the response was relatively flat at the
203 30 °C treatment (Fig. 1). The maximum values of the expectations occurred at a pH of 7.49
204 (Fig. 1C), 7.78 (Fig. 1D), and 7.37 (Fig. 1E) for the 10 °C, 20 °C, and 30 °C treatments,
205 respectively. The NPR at these values were 0.910 (0.76 to 1.06) mg O_2 g_{ww}^{-1} min^{-1}, 2.17 (1.94 to
206 2.40) mg O_2 g_{ww}^{-1} min^{-1}, and 2.03 (1.85 to 2.22) mg O_2 g_{ww}^{-1} min^{-1} at temperatures of 10 °C,
207 20 °C, and 30 °C, respectively.

208 Response of RGR to CO_2 concentration and pH

209 The response of RGR to CO_2 concentration and pH were similar to that of NPR, however in
210 general the 95% highest density credible intervals of the expectations were much wider (Fig. 2).
211 Therefore, the differences in the leave-one-out cross validation between a global model and a
212 model that fitted individual curves to each temperature treatment were relatively small in
213 magnitude. For example, these values were -15.8 ± 4.2 for the model evaluating the response
214 of RGR to CO_2 concentration and -13.7 ± 363 when the covariate was pH; all results indicated
215 that the more complex model better predicted the observations. Unlike NPR, the RGR was
216 highest at the 20 °C treatment, which was 0.57 ± 0.16 (n = 9). The RGR at the 10 °C treatment
217 was 0.24 ± 0.13 (n = 8) and at the 30 °C treatment was 0.50 ± 0.16 (n = 8).

218 The response of the expectations of the model with the CO_2 covariate was similar across
219 temperature treatments, with RGR increasing with increasing CO_2 concentrations then declining
220 over a broad range above a threshold concentration that differed with temperature treatment.
221 The maximum expected value of RGR for the 10 °C treatment occurred at 0.53 µatm and was
222 0.41 (0.26 to 0.57) day^{-1} (Fig. 2A). The maximum expected value for the 20 °C treatment was
223 observed at 1.39 µatm and was 0.69 (0.53 to 0.85) day^{-1} (Fig. 2B) and for the 30 °C treatment,
224 the maximum value was observed at 2.46 µatm and was 0.65 (0.48 to 0.82) day^{-1} (Fig. 2C).

225 The response of RGR with respect to pH was similar to CO_2. The curves were all dome-shaped,
226 with peaks occurring between pH of 6.4 to 7.9. For the 10 °C temperature treatment, maximum
227 values of expected RGR occurred at a pH of 7.9 and was 0.49 (0.05 to 1.18) day^{-1} (Fig. 2D). At

the 20 °C temperature treatment, the peak occurred at a pH of 6.6 and the maximum expected value was 0.67 (0.53 to 0.83) day^{-1} (Fig. 2E). At the highest temperature treatment of 30 °C, the peak occurred at a pH of 6.4 and the maximum expected value of RGR was 0.65 (0.48 to 0.82) day^{-1} (Fig. 2F).

Discussion

We show that interactive effects between dissolved CO_2 concentration and temperature on both the net photosynthesis and relative growth rate of cultivated *Ulva prolifera* germling clusters. The first key finding is that the optimal CO_2 concentration required to maximize RGR is temperature-dependent, increasing from about 0.53 µatm at 10 °C to 1.39 µatm at 20 °C and 2.46 µatm at 30 °C. The second key finding is that the response of the relative growth rates and net photosynthesis rates of the germling clusters were dissimilar (Fig. 1 and Fig. 2). In the case of RGR a unimodal response was clearly detected, however the response of NPR was linear in nature; nevertheless, peak expected values of NPR were detected at 0.19 µatm at 10 °C decreasing to 0.02 µatm and 0.06 µatm at 20 °C and 30 °C, respectively. Another important finding of this study was that the responses of RGR and NPR with respect to the covariate used in the GAM were also dissimilar, where responses appeared unimodal and monotonic.

We suggest several hypotheses to explain the divergence between conditions optimizing short-term NPR and long-term RGR. While NPR tended to peak around pH 7.5 to 7.8 (Fig. 1), which coincides with the maximum calculated bicarbonate (HCO_3^-) availability, RGR optima occurred at different, often lower, pH values depending on temperature (Fig. 2). This discrepancy highlights that maximizing instantaneous carbon fixation does not necessarily translate directly to maximizing growth over longer periods. Several factors likely contributed to this discrepancy. RGR integrates metabolic activity over the full 24-hour cycle, including dark respiration, which may respond differently than photosynthesis to changes in pH and DIC speciation. Secondly, *U. prolifera* is believed to possess carbon concentrating mechanisms (CCMs), and therefore, the germling clusters may have boosted carbon fixation, at the cost of consuming more energy (Raven et al. 2000; Hopkinson et al. 2011). Diverting energy to operating a CCM might have diverted resources from growth, hence potentially becoming less efficient. Thirdly, compared to the short-term experiments to assess NPR, the RGR experiments may have allowed the germling clusters to acclimate to the environmental conditions leading to physiological adjustments in enzyme activity, membrane transport, and carbon allocation that

are not captured in short-term assessments of NPR (Fernández et al. 2014). Finally, while elevated CO_2 enhances carbon supply, growth can be affected by nutrient concentrations; perhaps the pH dependence of the efficiency of nutrient uptake is another factor that should be explored in future experiments (Young et al. 2016). In this study, RGR was a more integrated measure of performance and is more relevant for predicting biomass yield in cultivation.

The observed peak in NPR around pH 7.5-7.8 (Fig. 2), where HCO_3^- dominates DIC speciation, is consistent with the known ability of *Ulva* species to efficiently utilize bicarbonate via active CCMs (Giordano et al. 2005; Raven et al. 2014). *U. prolifera* possesses pyrenoids (Cui et al. 2018) and exhibits evidence of C_4-like metabolism and active HCO_3^- uptake, likely involving carbonic anhydrases (CAs) and specific transporters (Xu et al. 2012; Liu et al. 2020; Young et al. 2021; Zhang et al. 2024). It is relevant to note that the efficiency of these mechanisms can be influenced by the diffusive boundary layer and external pH, since boundary layer effects reduce mass flux into the germling cluster (Cornwall et al. 2017). Indeed, for the strain that was studied here, NPR and RGR was highest when the molar fraction of HCO_3^- was highest. Which provides additional support to past studies (e.g., Xu et al. 2012; Liu et al. 2020; Young et al. 2021; Zhang et al 2024) that hypothesize that *U. prolifera* possess a CCM. While optimal HCO_3^- availability appears beneficial for short-term photosynthesis, the decline in RGR at very high CO_2 concentrations (and correspondingly low pH, Fig. 1 and 2) suggests potential negative impacts. These could include direct pH stress affecting membrane integrity or enzyme function, increased energetic costs of maintaining intracellular pH homeostasis, or potential down-regulation of CCM components when external CO_2 is saturating (Hepburn et al. 2011). This study was not designed to elucidate CCM mechanisms and pH stress; clearly more work is needed to elucidate the details suggested here and we expect that such insight will further enhance the production of this species.

Temperature is a fundamental factor that modulates physiological responses. The higher overall RGR at 20 °C and 30 °C compared to 10 °C supports previous findings for *U. prolifera* (Xiao et al. 2016; Cui et al. 2015). The shift in the optimal CO_2 concentration for RGR towards higher levels at higher temperatures likely reflects increased metabolic demand for carbon driven by temperature-dependent enzyme kinetics (including Rubisco) and overall higher metabolic rates (Duke et al. 1989; Terada et al. 2016). The maintenance of relatively high NPR at 30 °C across various CO_2 concentrations (Fig. 1C) was somewhat higher than expected from some previous studies on wild populations (e.g., Xiao et al. 2016) and might reflect the physiological characteristics of the specific cultivated strain (Sato et al. 2021) that was used in this study or a

292 protective effect of high DIC supply mitigating photorespiration or thermal stress under the
293 experimental conditions (Ehleringer et al. 1997).

294 The response of the expected values of NPR was not uniform across temperature treatments. At
295 20 °C, NPR was weakly dependent on CO_2 concentration, whereas at 30 °C NPR the
296 dependence on CO_2 was not clear in the model results. This may be because of the increasing
297 pH (i.e., increasing alkalinity) and its effect on NPR. As mentioned above, pH stress affects the
298 integrity of cellular membranes and may influence the function of enzymes associated in
299 photosynthesis and for high temperatures we hypothesize that these effects were magnified.
300 Regardless of these potential stresses, NPR remained high throughout a wide range of pH (and
301 CO_2 concentrations) at the 20 °C and 30 °C temperature treatments.

302 Our findings confirm previous reports that CO_2 enrichment enhances *U. prolifera* growth (Xu &
303 Gao 2012; Sun et al. 2021; Wang et al. 2021). However, the observed RGR values observed
304 here (peaking at 0.24 to 0.57 day^{-1}) were substantially higher than some reports (e.g., Wang et
305 al. 2021 reported 0.25 to 0.29 day^{-1}). As suggested above, this difference may be due to
306 laboratory conditions, the strain used in this study (Sato et al. 2021), and perhaps the germling
307 cluster method, which was developed to optimize production yield (Hiraoka & Oka 2008).
308 Nevertheless, growth rates in Ulva are known to be highly variable depending on strain and
309 conditions and more research is needed to make precise and accurate conclusions on how RGR
310 is influenced by environmental conditions (Lawton et al. 2013; Fort et al. 2019).

311 Crucially, this study provides temperature-specific CO_2 optima for RGR. For land-based
312 cultivation aiming to maximize biomass yield using this strain, enriching CO_2 to achieve
313 dissolved concentrations around 1.39 µatm (pH 6.6) at 20 °C, or 2.76 µatm (pH 6.4) at 30 °C,
314 appears highly beneficial. Based on the GAM predictions, these optimal conditions resulted in
315 RGRs approximately 1.5 times higher than control (ambient CO_2) conditions, regardless of
316 temperature. However, exceeding these optima leads to diminishing returns and eventual growth
317 inhibition, highlighting the need for careful control. Implementing such enrichment requires
318 systems to monitor the CO_2 concentration and/or pH as well as assessing the costs associated
319 with implementation (Milledge & Harvey 2016; O'Brien et al. 2022). We emphasize that CO_2
320 enrichment is not a general strategy for yield enhancement; optimal levels must be adjusted
321 based on the water temperature, as well as cultivar strain and likely other environmental factors.

322 This study was conducted under controlled laboratory conditions using a single, albeit
323 commercially relevant, strain of *U. prolifera*. Responses may differ in outdoor systems with

fluctuating light and nutrient availability, or for other strains. The carbonate system was not fully characterized (e.g., Total Alkalinity was not measured), relying on calculated HCO_3^- fractions based on measured pH, temperature, and salinity. Future work could benefit from measuring additional carbonate parameters for a more precise understanding of DIC speciation. Furthermore, the mechanisms underlying the NPR vs. RGR discrepancy warrant further investigation, potentially involving measurements of respiration, nutrient uptake kinetics, and enzyme activities under different long-term CO_2/pH regimes.

In conclusion, the optimal dissolved CO_2 concentration for maximizing the relative growth rate of *Ulva prolifera* germling clusters is appears to be dependent on water temperature, increasing from about 0.53 µatm at 10 °C to 2.46 µatm at 30 °C under the tested conditions. Achieving these temperature-specific optima is likely to enhance biomass production compared to ambient CO_2 levels. These findings provide quantitative data for optimizing CO_2 enrichment protocols in terrestrial aquaculture of *U. prolifera*, and should be able to contribute to the development of more efficient and economically viable seaweed cultivation systems. The study also serves as a reminder that the physiological response of macroalgae is complex and simply optimizing short-term photosynthesis does not always equate to optimizing long-term growth, emphasizing the need for integrated assessments when developing cultivation strategies.

References

Badger MR, Kaplan A, Berry JA (1980) Internal inorganic carbon pool of *Chlamydomonas reinhardtii*. Plant Physiol 66:407–413. https://doi.org/10.1104/pp.66.3.407

Bolton JJ, et al. (2016) Seaweed biorefinery: a sustainable source of biomass and bio-products. In: Fleurence J, Levine I (eds) Seaweed in Health and Disease Prevention. Academic Press, pp 267-287. https://doi.org/10.1016/B978-0-12-802772-1.00011-9

Bruhn A, et al. (2011) Bioenergy potential of *Ulva lactuca*: biomass yield, methane production and combustion. Bioresour Technol 102(3):2595-2604. https://doi.org/10.1016/j.biortech.2010.10.019

Chinnasamy S, Ramakrishnan B, Bhatnagar A, Das K (2009) Biomass production potential of a wastewater alga chlorella vulgaris arc 1 under elevated levels of CO_2 and temperature. Int J Mol Sci 10(2):518–532. https://doi.org/10.3390/ijms10020518

353 Cornwall CE, et al. (2017) Diffusion boundary layers modify the effectiveness of favoured CO_2-
354 concentrating mechanisms in calcifying and non-calcifying macroalgae. J Exp Bot
355 68(14):3947–3959. https://doi.org/10.1093/jxb/erx199

356 Cui J, et al. (2015) Adaptability of free-floating green tide algae in the Yellow Sea to variable
357 temperature and light intensity. Mar Pollut Bull 101(2):660–666.
358 https://doi.org/10.1016/j.marpolbul.2015.10.033

359 Cui J, et al. (2018) Taxonomic reassessment of *Ulva prolifera* (Ulvophyceae, Chlorophyta)
360 based on specimens from the type locality and Yellow Sea green tides. Phycologia 57(6):692–
361 704. https://doi.org/10.2216/17-139.1

362 Dan A, Hiraoka M, Ohno M (1998) On the induction of reproductive cell formation in the green
363 alga, *Enteromorpha prolifera*: Relationship of temperature and size of tissue disk. Aquac Sci
364 46(4):503-508.

365 Dan A, Ohno M, Matsuoka M (1997) Cultivation of green alga *Enteromorpha prolifera* using
366 chopped tissue for artificial seeding. Aquac Sci 45(1):5-8.

367 Dickson AG, Sabine LC, Christian JR (2007) Guide to best practices for ocean CO_2
368 measurements. PICES Special Publication 3: 1-191.

369 Duke CS, Litaker W, Ramus J (1989) Effect of temperature on nitrogen-limited growth rate and
370 chemical composition of *Ulva curvata* (Ulvales: Chlorophyta). Mar Biol 100(2):143–150.
371 https://doi.org/10.1007/BF00391953

372 Ehleringer JR, Cerling TE, Helliker BR (1997) C_4 photosynthesis, atmospheric CO_2, and
373 climate. Oecologia 112(3):285–299. https://doi.org/10.1007/s004420050311

374 Fernández PA, et al. (2014) Exploring the photosynthetic strategy for acclimation to low-pH
375 conditions in *Ulva rigida* (Chlorophyta). J Phycol 50(6):1051-1061.
376 https://doi.org/10.1111/jpy.12239

377 Figueroa FL, et al. (2021) Effects of CO_2 enrichment on the ecophysiology of *Ulva rigida* and
378 *Ulva rotundata* from Southern Spain. J Appl Phycol 33:1809–1821.
379 https://doi.org/10.1007/s10811-021-02414-2

380 Fort A, et al. (2019) Extensive variations in diurnal growth patterns and metabolism among

Ulva spp. strains. Plant Physiol 180(1):109–123. https://doi.org/10.1104/pp.18.01513

Fort A, Mannion C, Fariñas-Franco JM, Sulpice R (2020) Green tides select for fast expanding Ulva strains. Sci Total Environ 698:134337. https://doi.org/10.1016/j.scitotenv.2019.134337

Gao K, Aruga Y, Asada K, Ishihara T, Akano T, Kiyohara M (1991) The effects of enriched CO_2 concentration on the growth and photosynthesis of unicellular marine algae. Acta Bot Sin 33(7):549-556.

Gao X, Endo H, Agatsuma Y (2015) Effect of increased seawater temperature on biomass, growth, and maturation of *Saccharina japonica* near its southern limit in northern Japan. J Appl Phycol 27(3):1263–1270. https://doi.org/10.1007/s10811-014-0417-0

Gattuso J-P, Epitalon J-M, Lavigne H, Orr J (2024) seacarb: Seawater Carbonate Chemistry. R package version 3.3.3. https://CRAN.R-project.org/package-seacarb.

Giordano M, Beardall J, Raven JA (2005) CO_2 concentrating mechanisms in algae: Mechanisms, environmental modulation, and evolution. Annu Rev Plant Biol 56(1):99–131. https://doi.org/10.1146/annurev.arplant.56.032604.144052

Harley CDG, et al. (2012) The impacts of climate change in coastal marine systems. Ecol Lett 15(11):1300-1315. https://doi.org/10.1111/j.1461-0248.2012.01831.x

Hepburn CD, et al. (2011) Physiological responses of macroalgae to ocean acidification: implications for macroalgal aquaculture. Aquac Environ Interact 1(3):177-189. https://doi.org/10.3354/aei00019

Hiraoka M, Dan A, Hagihira M, Ohno M (1999) Growth and maturity of clonal thalli in *Enteromorpha prolifera* under different temperature conditions. Nippon Suisan Gakkaishi 65(2):302-303. https://doi.org/10.2331/suisan.65.302

Hiraoka M, Higa M (2016) Novel distribution pattern between coexisting sexual and obligate asexual variants of the true estuarine macroalga *Ulva prolifera*. Ecol Evol 6(11):3658–3671. https://doi.org/10.1002/ece3.2149

Hiraoka M, Kinoshita Y, Higa M, Tsubaki S, Monotilla AP, Onda A, Dan A (2020) Fourfold daily growth rate in multicellular marine alga *Ulva meridionalis*. Sci Rep 10(1):12606. https://doi.org/10.1038/s41598-020-69536-4

409 Hiraoka M, Oka N (2008) Tank cultivation of *Ulva prolifera* in deep seawater using a new
410 "germling cluster" method. J Appl Phycol 20(1):97–102. https://doi.org/10.1007/s10811-007-
411 9186-3

412 Hopkinson BM, et al. (2011) The energetic cost of acquiring carbon by marine phytoplankton.
413 New Phytol 190(3):522-534. https://doi.org/10.1111/j.1469-8137.2010.03593.x

414 Jiang J, Yu Y, Chen Y, Li Y, Xu N (2024) Photoperiod mediates the effects of temperature and
415 light intensity on the proliferation of *Ulva prolifera*. J Ocean Univ China 23(1):255–263.
416 https://doi.org/10.1007/s11802-024-5473-8

417 Lavoie M, Le Faucheur S, Boullemant A, Fortin C, Campbell PGC (2012) The influence of ph
418 on algal cell membrane permeability and its implications for the uptake of lipophilic metal
419 complexes. Journal of Phycology 48: 293-302. https://doi.org/10.1111/j.1529-
420 8817.2012.01126.x

421 Lawton RJ, Mata L, De Nys R, Paul NA (2013) Algal bioremediation of waste waters from
422 land-based aquaculture using Ulva: Selecting target species and strains. PLoS ONE
423 8(10):e77344. https://doi.org/10.1371/journal.pone.0077344

424 Lawton RJ, Sutherland JE, Glasson CRK, Magnusson ME (2021) Selection of temperate Ulva
425 species and cultivars for land-based cultivation and biomass applications. Algal Res 56:102320.
426 https://doi.org/10.1016/j.algal.2021.102320

427 Lin A-P, et al. (2011) Diluted seawater promoted the green tide of *Ulva prolifera* (Chlorophyta,
428 Ulvales). Phycol Res 59(4):295–304. https://doi.org/10.1111/j.1440-1835.2011.00629.x

429 Liu D, et al. (2013) The world's largest macroalgal bloom in the Yellow Sea, China: formation
430 and implications. Estuar Coast Shelf Sci 129:2-10. https://doi.org/10.1016/j.ecss.2013.05.021

431 Liu D, et al. (2020) Role of C4 carbon fixation in *Ulva prolifera*, the macroalga responsible for
432 the world's largest green tides. Commun Biol 3(1):494. https://doi.org/10.1038/s42003-020-
433 01225-4

434 Mantri VA, et al. (2021) Land-based seaweed cultivation: A sustainable alternative approach.
435 Rev Aquac 13(4):2236-2254. https://doi.org/10.1111/raq.12572

436 Meyer MT, Whittaker C, Griffiths H (2017) The algal pyrenoid: Key unanswered questions. J

437 Exp Bot 68(14):3739–3749. https://doi.org/10.1093/jxb/erx178

438 Milledge JJ, Harvey PJ (2016) Potential process 'hurdles' in the use of macroalgae as feedstock
439 for biofuel production in the British Isles. J Chem Technol Biotechnol 91(8):2221–2234.
440 https://doi.org/10.1002/jctb.5003

441 Millero FJ, Graham TB, Huang F, Bustos-Serrano H, Pierrot D (2006) Dissociation constants of
442 carbonic acid in seawater as a function of salinity and temperature. Mar Chem 100(1–2):80–94.
443 https://doi.org/10.1016/j.marchem.2005.12.001

444 Nakamura M, et al. (2020) Photosynthesis and growth of *Ulva ohnoi* and *Ulva pertusa*
445 (Ulvophyceae) under high light and high temperature conditions, and implications for green tide
446 in Japan. Phycol Res 68(2):152–160. https://doi.org/10.1111/pre.12410

447 Nardelli AE, et al. (2021) Cultivation of *Ulva ohnoi* in pilot scale for bioremediation and
448 biomass production using aquaculture wastewater. J Appl Phycol 33:3167–3179.
449 https://doi.org/10.1007/s10811-021-02503-2

450 O'Brien KR, et al. (2022) A review of CO_2 supplementation in algal cultivation: bottlenecks and
451 opportunities. Algal Res 64:102671. https://doi.org/10.1016/j.algal.2022.102671

452 Ohno M, Mizutani S, Taino S, Takahashi I (1999) Ecology of the edible green alga
453 *Enteromorpha prolifera* in Shimanto river Southern Japan. Bull Mar Sci Fish Kochi Univ
454 19:27-35.

455 Weiss R (1974) Carbon dioxide in water and seawater: the solubility of a non-ideal gas. Mar
456 Chem 2: 203-215.

457 Park CS, Hwang EK (2011) An investigation of the relationship between sediment particles size
458 and the development of green algal mats (*Ulva prolifera*) on the intertidal flats of Muan, Korea.
459 J Appl Phycol 23(3):515–522. https://doi.org/10.1007/s10811-010-9620-9

460 Park J, et al. (2024) Harnessing green tide Ulva biomass for carbon dioxide sequestration. Rev
461 Environ Sci Bio/Technol 23(4):1041–1061. https://doi.org/10.1007/s11157-024-09705-3

462 Pedersen EJ, Miller DL, Simpson GL, Ross N (2019) Hierarchical generalized additive models
463 in ecology: an introduction with mgcv. PeerJ 7:e6876. https://doi.org/10.7717/peerj.6876

464 R Core Team (2024) R: A language and environment for statistical computing. R Foundation

for Statistical Computing, Vienna, Austria. URL https://www.R-project.org/.

Raven JA, et al. (2000) The costs of acquiring carbon by marine autotrophs. In: Press MC, Scholes JD, Barker MG (eds) Physiological Plant Ecology. Springer, Dordrecht, pp 21-48. ISBN: 978-94-011-4207-1

Raven JA, et al. (2014) Inorganic carbon acquisition by marine autotrophs. Adv Bot Res 71:87-153. https://doi.org/10.1016/B978-0-12-800144-7.00003-6

Raven JA, Girard-Bascou J (2001) Algal model systems and the elucidation of photosynthetic metabolism. J Phycol 37(6):943–950. https://doi.org/10.1046/j.1529-8817.2001.01079.x

Sato Y (2024) Cultivation of seaweed in land-based tank system in Japan. Agric Biotechnol 8(9): 744-474.

Sato Y, et al. (2021) Different growth and sporulation responses to temperature gradient among obligate apomictic strains of *ulva prolifera*. Plants 10(11):2256. https://doi.org/10.3390/plants10112256

Shimada S (2012) The role of algae in climate change. In: Watanabe M (Ed.). Handbook of Algae: Their Diversity and Utilization, pp 564-567.

Sun J, et al. (2021) Elevated CO_2 influences competition for growth, photosynthetic performance and biochemical composition in *Neopyropia yezoensis* and *Ulva prolifera*. Algal Res 56:102313. https://doi.org/10.1016/j.algal.2021.102313

Taiz L, Zeiger E (2017) Photosynthesis: Physiological and ecological considerations. In: Plant physiology and development, 6th ed. Sinauer Associates, pp 245-265.

Terada R, et al. (2016) The effect of irradiance and temperature on the photosynthesis and growth of a cultivated red alga *Kappaphycus alvarezii* (Solieriaceae) from Vietnam, based on *in situ* and *in vitro* measurements. J Appl Phycol 28(1):457–467. https://doi.org/10.1007/s10811-015-0557-x

Toyokawa C, Yamano T, Fukuzawa H (2020) Pyrenoid starch sheath is required for LCIB localization and the CO_2-concentrating mechanism in green algae. Plant Physiol 182(4):1883–1893. https://doi.org/10.1104/pp.19.01587

Uribe EG, Jagendorf AT (1967) On the localization of organic acids in acid-induced ATP

493 synthesis. Plant Physiol 42(5):697–705. https://doi.org/10.1104/pp.42.5.697

494 Vehtari A, Gelman A, Gabry J (2017) Practical Bayesian model evaluation using leave-one-out
495 cross-validation and WAIC. Stat Comput 27(5):1413–1432. https://doi.org/10.1007/s11222-
496 016-9696-4

497 Wang Y, et al. (2021) Elevated CO_2 accelerated the bloom of three Ulva species after one life
498 cycle culture. J Appl Phycol 33(6):3963–3973. https://doi.org/10.1007/s10811-021-02562-5

499 Watanabe F, et al. (1999) Dried green and purple lavers (Nori) contain substantial amounts of
500 biologically active vitamin b(12) but less of dietary iodine relative to other edible seaweeds. J
501 Agric Food Chem 47(6):2341–2343. https://doi.org/10.1021/jf981065c

502 Wood SN (2011) Fast stable restricted maximum likelihood and marginal likelihood estimation
503 of semiparametric generalized linear models. J R Stat Soc Series B Stat Methodol 73(1):3–36.
504 https://doi.org/10.1111/j.1467-9868.2010.00749.x

505 Xiao J, et al. (2016) Effect of temperature, salinity and irradiance on growth and photosynthesis
506 of *Ulva prolifera*. Acta Oceanol Sin 35(10):114–121. https://doi.org/10.1007/s13131-016-0891-
507 0

508 Xu J, Gao K (2012) Future CO_2-induced ocean acidification mediates the physiological
509 performance of a green tide alga. Plant Physiol 160(4):1762–1769.
510 https://doi.org/10.1104/pp.112.206961

511 Xu J, et al. (2012) Evidence of coexistence of C_3 and C_4 photosynthetic pathways in a green-
512 tide-forming alga, *Ulva prolifera*. PLoS ONE 7(5):e37438.
513 https://doi.org/10.1371/journal.pone.0037438

514 Ye N H, et al. (2011) 'Green tides' are overwhelming the coastline of our blue planet: The
515 world's largest example. Ecol Res 26(3):477-485. https://doi.org/10.1007/s11284-011-0800-1

516 Young CS, et al. (2016) Effects of temperature and nutrient concentration on the growth and
517 nutrient uptake of different Ulva species. J Appl Phycol 28:2939–2948.
518 https://doi.org/10.1007/s10811-016-0829-y

519 Young EB, et al. (2021) Carbonic anhydrase activity and inorganic carbon acquisition in bloom-
520 forming Ulva species. Photosynth Res 147(3):329-342. https://doi.org/10.1007/s11120-021-

00823-5

Zhang X, et al. (2024) The contribution of biophysical and biochemical CO_2 concentration mechanisms to the carbon fixation of the green macroalga *Ulva prolifera*. Mar Life Sci Technol. https://doi.org/10.1007/s42995-024-00265-7

Zou D (2005) Effects of elevated atmospheric CO_2 on growth, photosynthesis and nitrogen metabolism in the economic brown seaweed, *Hizikia fusiforme* (Sargassaceae, Phaeophyta). Aquaculture 250(3–4):726–735. https://doi.org/10.1016/j.aquaculture.2005.05.014

Funding Declaration

This study was funded by FY2023-2024 Miyagi Carbon Dioxide Emission Reduction Project Subsidy (Research and Development Category)].

Table 1 The eight target CO_2 concentrations measured with the CGP-31 meter (mg L^{-1}) and converted to µatm using the seacarb package in R. The initial and final CO_2 concentrations and pH were determined before and after the photosynthesis experiments. Values are the mean (one standard deviation) of 15 samples. There are only a total of 14 samples when CO_2 is 5.24 mg L^{-1} (0.42 µatm) and pH is 7.41).

CO_2 (mg L^{-1})		CO_2 (µatm)		pH (-)	
Initial	Final	Initial	Final	Initial	Final
1.03 (0.14)	0.78 (0.07)	0.08 (0.01)	0.06 (0.01)	7.92 (0.06)	8.15 (0.06)
5.24 (1.38)	3.29 (1.66)	0.42 (0.11)	0.27 (0.14)	7.41 (0.11)	7.60 (0.20)
16.83 (1.67)	9.95 (1.97)	1.36 (0.14)	0.80 (0.17)	6.93 (0.09)	7.16 (0.11)
25.00 (2.54)	15.53 (1.84)	2.01 (0.20)	1.25 (0.15)	6.81 (0.03)	6.98 (0.04)
35.67 (3.52)	24.43 (5.81)	2.87 (0.32)	1.97 (0.49)	6.69 (0.09)	6.79 (0.09)
46.67 (1.76)	32.13 (4.19)	3.75 (0.09)	2.59 (0.35)	6.64 (0.09)	6.70 (0.07)
87.00 (9.96)	65.27 (7.29)	7.00 (0.81)	5.25 (0.63)	6.34 (0.02)	6.41 (0.05)
131.67 (3.42)	103.73 (6.56)	10.59 (0.20)	8.35 (0.60)	6.16 (0.01)	6.27 (0.16)

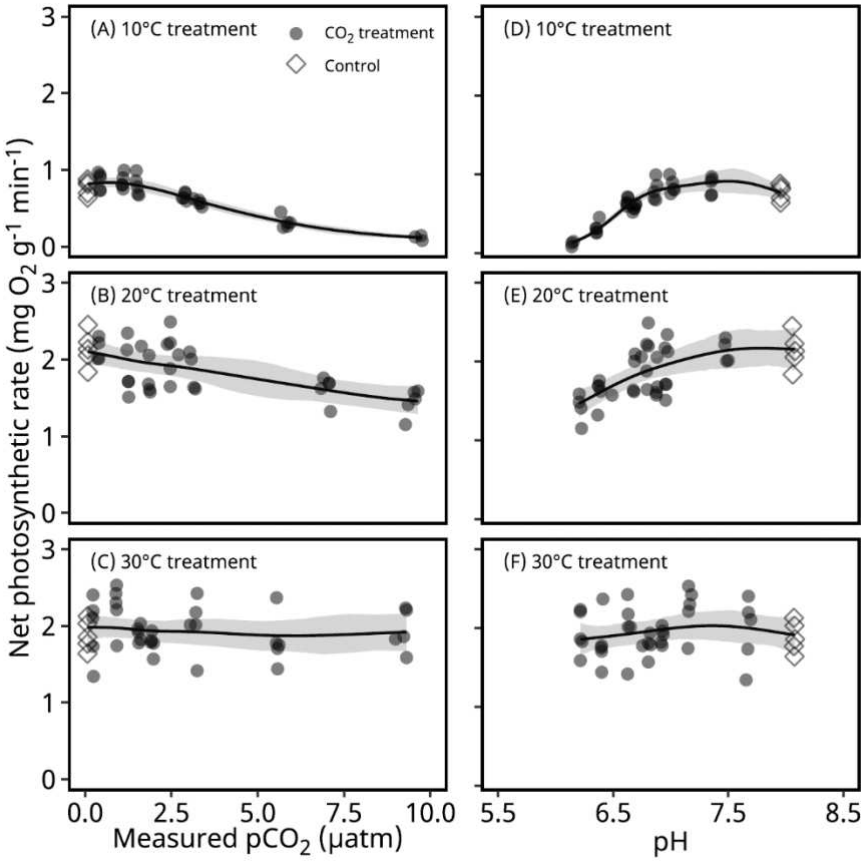
Table 2 The target CO_2 concentrations measured with the CGP-31 meter (mg L^{-1}) and converted to µatm using the seacarb package in R. Values indicate the mean (one standard deviation) CO_2 concentration and pH prior to start of the relative growth experiments. The conversion was done at 31 psu and 101.35 kPa. The samples (N) used to estimate CO_2 ranged from five to seven.

Temperature (°C)	CO_2 (mg L^{-1})	CO_2 (µatm)	pH (-)	N
10	0.5 (0.2)	0.04 (0.01)	8.62 (0.27)	5
10	4.4 (2.4)	0.36 (0.19)	7.17 (0.13)	7
10	13.6 (1.7)	1.12 (0.14)	6.75 (0.09)	7
10	23.6 (2.7)	1.94 (0.22)	6.55 (0.13)	7
10	36.3 (4.2)	2.99 (0.34)	6.33 (0.14)	7
10	56.5 (8.7)	4.65 (0.72)	6.18 (0.19)	5
10	96.1 (7.4)	7.92 (0.61)	5.87 (0.04)	5
10	143.1 (4.4)	11.78 (0.36)	5.74 (0.07)	5
20	2.1 (0.6)	0.17 (0.05)	8.28 (0.13)	6
20	8.3 (2.2)	0.67 (0.18)	6.93 (0.13)	7
20	16.4 (2.1)	1.33 (0.17)	6.65 (0.08)	7
20	22.6 (8.5)	1.84 (0.69)	6.77 (0.20)	6
20	24.5 (2.3)	2.00 (0.18)	6.49 (0.10)	7
20	37.1 (4.0)	3.02 (0.32)	6.35 (0.07)	7
20	64.5 (24.9)	5.25 (2.03)	6.35 (0.19)	6
20	100.3 (31.4)	8.17 (2.56)	6.09 (0.13)	6
20	142.4 (41.0)	11.60 (3.34)	5.94 (0.12)	6
30	0.3 (0.2)	0.03 (0.01)	8.31 (0.05)	5
30	4.4 (2.1)	0.35 (0.17)	7.33 (0.23)	7
30	16.5 (2.7)	1.32 (0.22)	6.73 (0.09)	7
30	27.3 (1.5)	2.18 (0.12)	6.57 (0.11)	7
30	38.4 (0.9)	3.07 (0.08)	6.43 (0.06)	7
30	52.0 (5.8)	4.15 (0.46)	6.20 (0.08)	5
30	100.6 (8.5)	8.04 (0.68)	5.94 (0.08)	5
30	140.2 (7.8)	11.20 (0.62)	5.81 (0.10)	5

549 **Fig. 1** The response of net photosynthesis rates varies with respect to three levels of water
550 temperature and a gradient of CO_2 concentrations and the associated pH. The symbols indicate
551 the observations, the line indicates the expected value of the model, and the shaded region
552 indicates the 95% credible interval of the expected values.

553 **Fig. 2** The response of relative growth rate varies with respect to three levels of water
554 temperature and a gradient of CO_2 concentrations and the associated pH. The symbols indicate
555 the observations, the line indicates the expected value of the model, and the shaded region
556 indicates the 95% credible interval of the expected values.

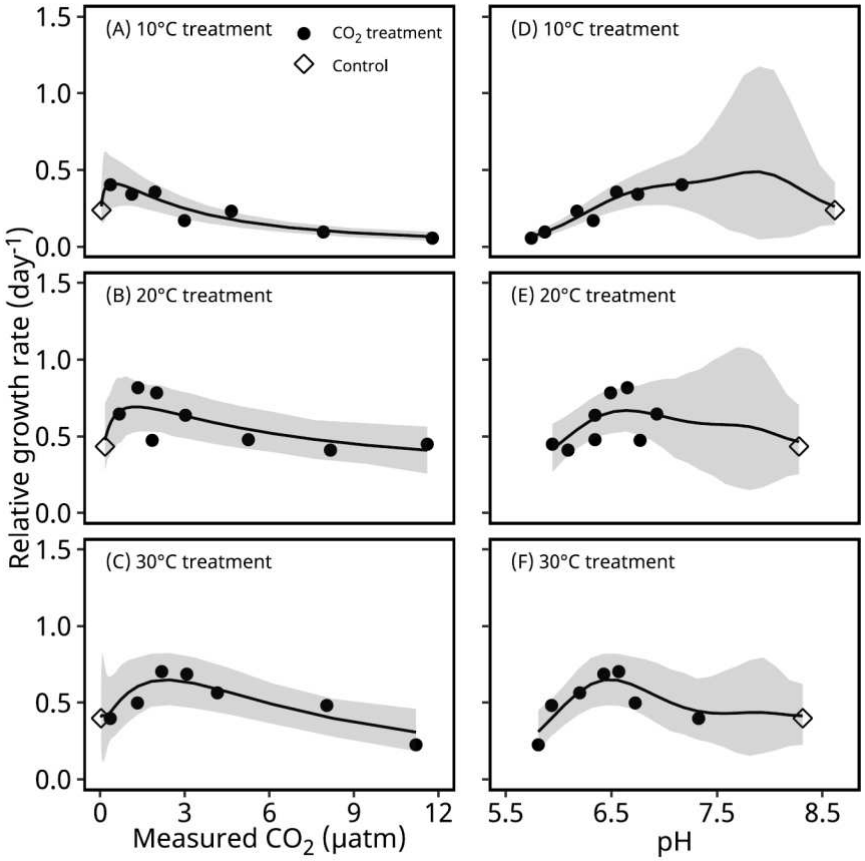
557 Figure 1



558

559

560 Figure 2



561

562